Journal of Magnetic Resonance 201 (2009) 57–60

Contents lists available at ScienceDirect

Journal of Magnetic Resonance

journal homepage: www.elsevier.com/locate/jmr

FID detection of EPR and ENDOR spectra at high microwave frequencies

H. Blok *, I. Akimoto [1], S. Milikisyants [2], P. Gast, E.J.J. Groenen, J. Schmidt

Huygens Laboratory, Department of Molecular Physics, Leiden University, P.O. Box 9504, 2300 RA Leiden, The Netherlands

ARTICLE INFO

Article history:
Received 23 December 2008
Revised 27 April 2009
Available online 15 August 2009

Keywords:
EPR
Pulsed EPR
High field
High-frequency
FID
ENDOR

ABSTRACT

High-frequency pulsed EPR spectroscopy allows FID detection of EPR spectra owing to the short dead time that can be achieved. This FID detection is particularly attractive for EPR and ENDOR spectroscopy of paramagnetic species that exhibit inhomogeneously broadened EPR lines and short dephasing times. Experiments are reported for the metalloprotein azurin at 275 GHz.

1. Introduction

The detection of EPR signals by the Free Induction Decay (FID) following an intense resonant microwave pulse has not seen a widespread application. This is in particular true for pulsed EPR studies of paramagnetic species in the condensed phase. The EPR lines of these systems usually exhibit inhomogeneous broadening by *g*-anisotropy or by unresolved or partly resolved hyperfine broadening. As a result the FID signal disappears on a time scale that is usually much shorter than the spectrometer dead time. This time scale is determined by the inhomogeneous line width Γ_{inh} or by the length of the excitation pulse. To obtain sufficiently long-lasting FID signals, transient spectral holes can be generated in the inhomogeneously broadened EPR line by applying a selective low-power pulse preceding the more intense detection pulse [1]. If the hole is sufficiently narrow the FID signal following this detection pulse will exceed the spectrometer dead time, provided that the relaxation times are sufficiently long. This FID-detected hole-burning allows the observation of EPR spectra [1], to discriminate between T_1 relaxation and spectral diffusion [1–3] and to measure hyperfine spectra [4,5]. The advantage of detection of the EPR spectra by the FID is that these are essentially free of distortions through nuclear modulations [1], in contrast to detection of the EPR spectra by the Electron Spin Echo (ESE). Nevertheless, the latter method is more generally used because of its experimental simplicity and the fact that it is free of dead-time artifacts.

Short dead times, which allow the detection of FID signals, are more easily obtained when single-mode cavities are used at high microwave frequencies, i.e., at frequencies of 95 GHz or higher. First, the microwave excitation power for the excitation pulses is relatively low, and secondly, the ringing time of the cavity is short because of the relatively broad bandwidth of its resonance curve. In this report we demonstrate that FID detection at 275 GHz makes it possible to record pulsed EPR and ENDOR spectra of paramagnetic systems with a dephasing time T_2 so short that detection by the ESE signal is impossible. This effect is illustrated for the metalloprotein azurin between 5.8 and 30 K. At 30 K the dephasing time of the unpaired copper spin of this protein is so short that ESE detection of the EPR spectrum is prohibited. In contrast, a strong FID-detected spectrum has been observed at this temperature with a signal-to-noise ratio (SNR) higher than 20. The FID signal benefits from the spin-locking effect in which the transient magnetization is locked along the driving B_1 field of the long and intense preparation pulse. The advantage of this method is that the transient magnetization relaxes with the spin–lattice relaxation time $T_{1\rho}$, which is considerably longer than the dephasing time T_2. In addition we show that also FID-detected ENDOR spectra can be obtained by adding an RF pulse and a short detection pulse following the preparation pulse.

2. Experimental

The FID-detected and ESE-detected EPR and ENDOR spectra were recorded with a home-built EPR spectrometer operating at 275 GHz. The typical microwave power incident on the cavity is 1 mW and the pulse length for a $\pi/2$-pulse is about 240 ns. This

* Corresponding author. Fax: +31 71 5275936.
E-mail address: huib@molphys.leidenuniv.nl (H. Blok).
[1] On leave from Wakayama University, Faculty of Systems Engineering, Wakayama, Japan.
[2] Present address: Rensselaer Polytechnic Institute, Department of Chemical Biology, Troy, NY, USA.

1090-7807/$ - see front matter © 2009 Elsevier Inc. All rights reserved.
doi:10.1016/j.jmr.2009.08.002

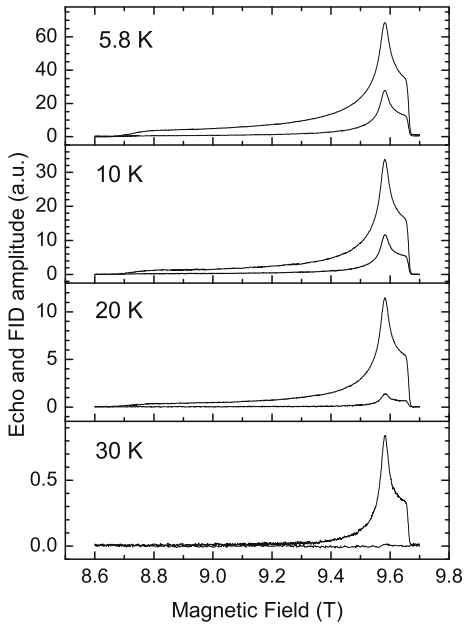

Fig. 1. Pulsed EPR spectra at 275 GHz of azurin at 5.8, 10, 20 and 30 K. The top spectrum in each panel concerns FID detection following a microwave pulse with a duration of 760 ns, using a gate of 50 ns, which opens 40 ns after the end of the microwave pulse. The weaker spectrum in each panel concerns electron-spin-echo detection following two pulses of 360 ns separated by 240 ns.

pulse is longer than mentioned in a previous publication due to small changes in the spectrometer [6]. The quality factor of the cavity is about 1000 and the dead time of about 30–40 ns following the microwave pulse is mainly caused by the trailing edge of the excitation pulse. For further details of the spectrometer we refer to [6,7].

Azurin from Pseudomonas aeruginosa was purified as described in Ref. [8]. The final concentration of azurin used for the experiments was 4.6 mM in 20 mM Hepes pH 7, containing 40% glycerol (v/v). For the ENDOR experiments a 4–5 times higher azurin concentration was used.

3. Results and discussion

In Fig. 1 the FID-detected and ESE-detected EPR spectra are presented of azurin at 275 GHz and temperatures ranging from 5.8 to 30 K. The FID-detected spectra have been obtained by applying a microwave pulse with duration of 760 ns and detecting the ensuing FID signal with an amplifier with a gate width of 50 ns that opens 40 ns after the termination of the excitation pulse. The ESE-detected spectra were obtained by applying two pulses of 360 ns separated by 240 ns. The spectra in Fig. 1 at 5.8 K show already the advantage of FID detection compared to ESE detection. The FID-detected spectrum has a SNR that is about 5 times larger than that of the ESE-detected spectrum, which suffers from the attenuation of the ESE signal in the time interval between the beginning of the first pulse and the formation of the echo, due to the dephasing time T_2 of 1.2 μs. The advantage of the FID detection is most striking for the EPR spectrum of azurin at 30 K. Here the ESE detection of the EPR spectrum is no longer possible because the dephasing time T_2 at this temperature is about 200 ns. In contrast, the FID-detected spectrum still exhibits a maximum SNR of about 20.

In Fig. 2 a simplified explanation of the remarkable behaviour of the FID signal is presented in a pictorial way in the rotating frame. Here the evolution of two spin packets with a resonance offset of $\pm\Delta B_0$ in the inhomogeneously broadened EPR line is depicted during the application of the resonant microwave pulse with amplitude B_1. After the beginning of the microwave pulse the two vectors representing the magnetization of these two spin packets start a precession around their effective fields B_{eff}. When the spins of these spin packets have fanned out in a time interval of the order of T_2 over the two cones there remain two components $M_0{}^{\text{L}}$ and

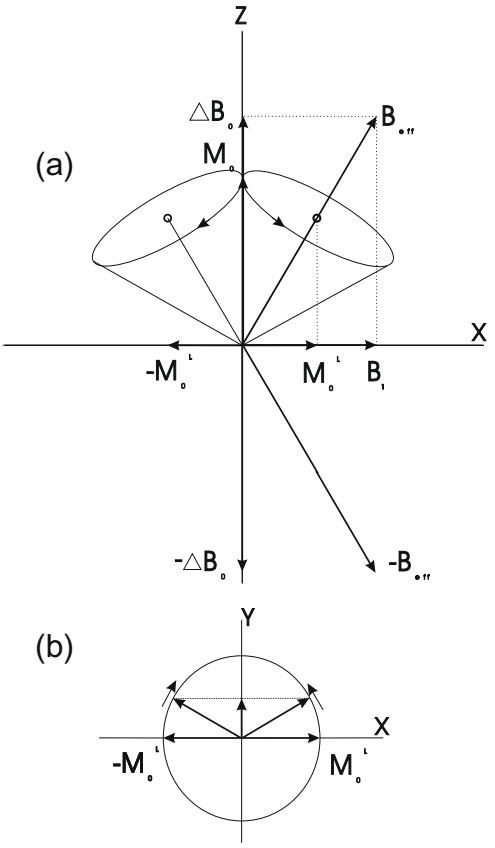

Fig. 2. (a) A pictorial representation of the evolution of two spin packets in the inhomogeneously broadened EPR line with off-resonance fields $\pm\Delta B_0$ during the application of an intense microwave pulse. (b) The evolution of the two locked components of the two spin packets in the x–y plane after the end of the microwave pulse.

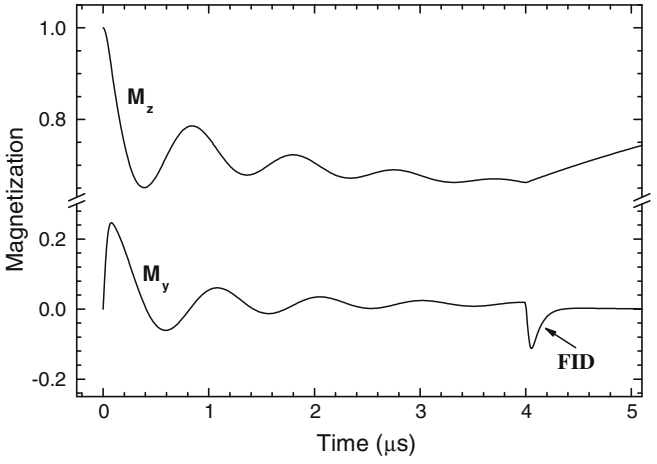

Fig. 3. Simulation of the evolution of the M_z and M_y components of the magnetization during and following a resonant microwave pulse at maximum microwave power and duration of 4 μs. The simulation parameters are those for the paramagnetic spins of azurin at 5.8 K, i.e., $T_1 = 4$ μs, $T_2 = 1.2$ μs, $\omega_1 = \gamma B_1 = 6.5$ rad s^{-1} and a line width $\Delta\omega = 30$ rad s^{-1}.

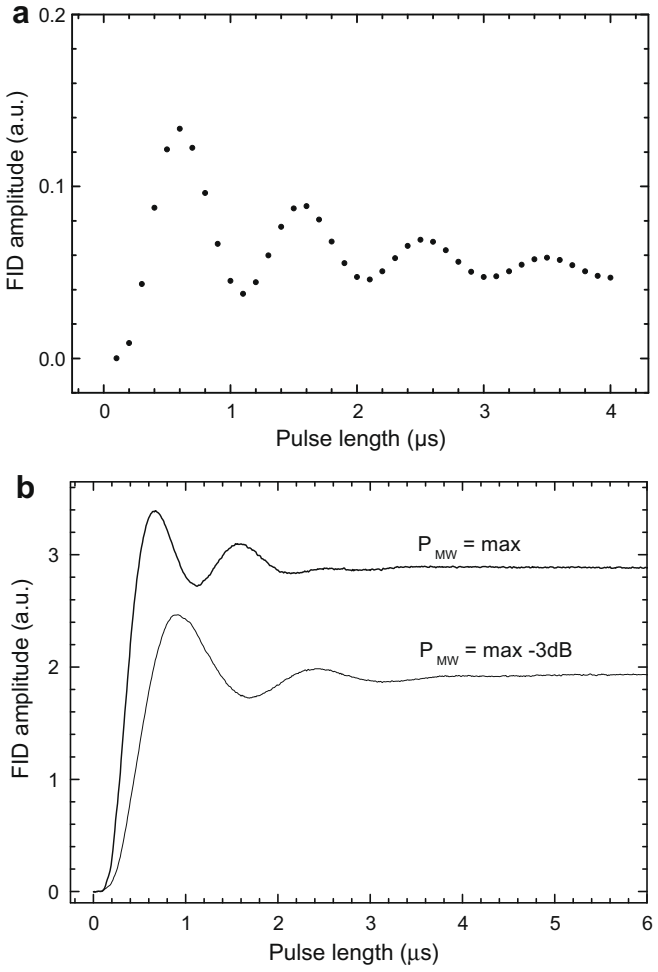

Fig. 4. (a) Simulation of the maximum amplitude of the FID signal, 50 ns after switching off the microwave pulse, as a function of the length of the microwave pulse. The data represent the result of 40 simulations by stepwise incrementing the pulse length by 100 ns from 100 to 4000 ns. The simulation parameters are the same as for Fig. 3. (b) The intensity of the FID signal for azurin at 9.59 T and 5.8 K as a function of the length of the resonant microwave pulse. The upper curve is obtained using the maximum microwave power of 1 mW incident on the cavity and the lower curve when this power has been reduced by 3 dB.

$-M_0{}^L$ "locked" parallel and anti-parallel to B_1. After the termination of the microwave pulse these two components start a precession, respectively, clockwise and anti-clockwise, in the x–y plane thus creating an oscillating magnetic component along the y-direction (Fig. 2b). The sum of the components of the various spin packets along B_1 forms the experimentally observed FID-type signal. This "spin-locking-induced FID" is much stronger than the ESE signal when the dephasing time T_2 is short, as demonstrated by the recordings at 30 K in Fig. 1. The spin-locked magnetization does not dephase during the application of the microwave pulse because it can only decay via spin–lattice relaxation processes characterized by a relaxation time $T_{1\rho}$ that is usually much longer than T_2. In contrast, in the ESE experiment, the induced magnetization dephases during the whole time interval of the ESE experiment.

To understand in more detail the evolution of the signals following a single microwave pulse, we have performed a numerical calculation, based on the Bloch equations, of the components M_z, M_y and M_x in the rotating frame using the values $T_2 = 1.2$ μs and $T_1 = T_{1\rho} = 4.0$ μs for azurin at $T = 5.8$ K and assuming an inhomogeneous line width of 30 MHz. The results for M_z and M_y are presented in Fig. 3. Of particular interest in this figure is the evolution of the component M_y, which is related to the experimentally observed signal. After the start of the microwave pulse at time $t = 0$ the M_y component grows to its maximum value in about 60–70 ns and subsequently evolves in an oscillatory way with a period of about 1000 ns. The important result of this simulation is the evolution of M_y after the termination of the microwave pulse. At the moment that this pulse is switched off at 4000 ns a rapid growth of M_y is observed, again in about 60–70 ns, followed by a decay with a time constant of about 150 ns. The rapid growth can be understood by considering the pictorial description in Fig. 2. At the moment the microwave pulse is switched off the components of the spin packets parallel and anti-parallel to B_1 cancel and it takes about a quarter of a precession period to create the maximum M_y component. This explains the fast increase of the FID signal immediately after the microwave pulse. This FID signal then disappears as a consequence of the spread in resonance fields of the spin packets, with a time constant of 150 ns as determined by the bandwidth of the excitation pulse. The oscillatory behaviour of M_y with a period of about 1000 ns during the microwave pulse results from an incomplete dephasing of the spin packets over their respective precession cones. This modulation has a frequency determined by the strength of the B_1 field and can be considered as an average Rabi nutation frequency. The advantage of the use of the spin-locking effect disappears when the spin–spin relaxation time T_2 is so short that the evolution of the magnetization, as illustrated in Fig. 2a, dies out before the spin-locked signal can develop. An estimate of the shortest T_2, that still allows an observable FID signal, is 50 ns.

In Fig. 4a the results are presented of the simulation of the maximum amplitude of the FID signal as a function of the length of the microwave pulse for stepwise increments of 100 ns. The simulation is in good agreement with the experimental observations in Fig. 4b. Here the maximum intensity of the FID signal for azurin at 9.59 T and $T = 5.8$ K is shown as a function of the length of the resonant microwave pulse. The FID signal does not reach a maximum value for a pulse length of 240 ns, which is the nominal value for a $\pi/2$-pulse, but for a pulse length of about 650 ns. After a few oscillations with a period of 1000 ns and for pulse lengths much longer than the dephasing time T_2, the FID signal approaches a constant value. The frequency of the oscillation depends on the applied microwave power as demonstrated by the recordings in Fig. 4b. The experimental curves in Fig. 4b

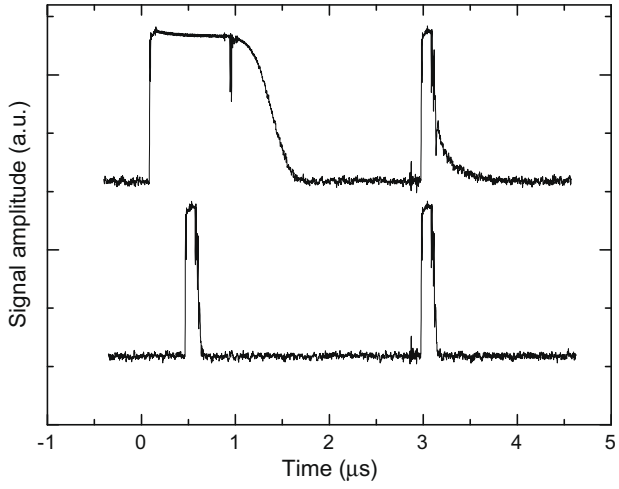

Fig. 5. The response to a long preparation pulse of 800 ns followed by a detection pulse of 100 ns at a delay of 2000 ns for azurin at 9.59 T and 4.5 K. A strong FID signal follows the short pulse. This FID is absent when the preceding saturating pulse is suppressed as shown in the lower graph.

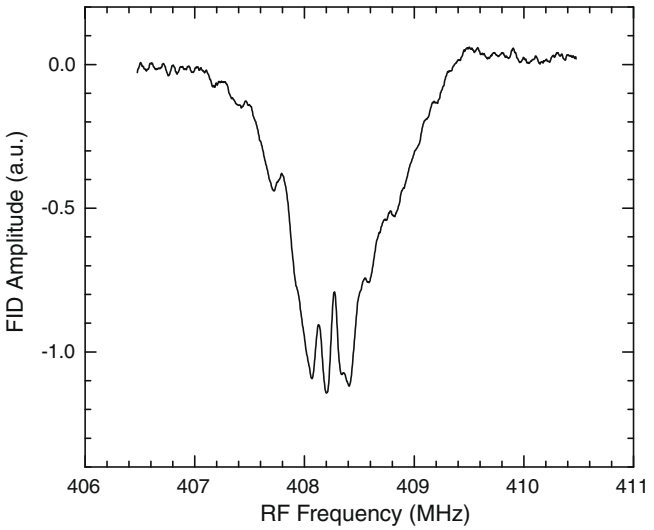

Fig. 6. The ^{1}H ENDOR spectrum of azurin at 9.59 T and 2 K as detected by the FID signal following the detection pulse as shown in Fig. 5. The spectrum has been obtained by applying an RF pulse between the preparation and the detection pulse and varying the RF frequency.

exhibit a shallower modulation pattern than the simulated curve. We attribute this difference to the inhomogeneity of the microwave B_1 field.

A further experiment on azurin, presented in Fig. 5, reveals a strong FID signal following a pulse with duration of 100 ns applied 2000 ns after a long preparation pulse. This FID signal is related to the spectral hole burnt by the preparation pulse into the inhomogeneously broadened EPR line, as shown by the evolution of M_z in Fig. 3. As demonstrated by Wacker et al. [1] a non-selective pulse, i.e., a pulse with high microwave power, produces a Fourier transform of the spectral hole burnt into an inhomogeneously broadened line by a preceding, non-selective, low-power pulse. In our case the short pulse has the same peak power as the preparation pulse. Nevertheless, the FID signal following the short pulse can be seen as an (incomplete) Fourier transform of the spectral hole. When this spectral hole is shifted or blurred, for instance by an RF pulse that saturates a nuclear transition, the intensity of the FID signal following the short pulse is affected [9]. This is shown in Fig. 6, where the ^{1}H ENDOR spectrum of azurin around 408 MHz is presented. This ENDOR spectrum has been obtained by applying an RF pulse between the preparation and the detection pulse, by varying the RF frequency and detecting the intensity of the FID signal following the second pulse.

The ^{1}H ENDOR spectrum presented in Fig. 6 is inhomogeneously broadened as a result of the partly random orientation of the excited spins of the azurin molecules. The homogeneous width of the ENDOR lines is expected to be determined by the nuclear dephasing times and not by the dephasing time of the electron spins. This aspect would represent an advantage of FID-detected ENDOR spectroscopy as compared to electron-spin-echo-envelope-modulation techniques. We plan to compare this ENDOR detection with related ENDOR detection schemes in a forthcoming paper.

4. Conclusion

Spin locking of the magnetization during long and intense microwave excitation pulses followed by detection of the FID is an attractive method to obtain EPR spectra of paramagnetic systems with a short dephasing time T_2. This method works especially well at high microwave frequencies, using single-mode resonators, where FID signals can be observed 40–50 ns after the termination of the microwave pulse. The FID detection of spectra is illustrated for paramagnetic systems with a dephasing time T_2 of 200 ns, where ESE detection fails. In addition ENDOR spectra have been observed by detecting the FID signal following a second non-selective microwave pulse and an RF pulse to saturate the nuclear transitions.

Acknowledgments

This work was supported with financial aid of The Netherlands Organization for Scientific Research (NWO), Department Chemical Sciences (CW). I. A. was supported by the Fellowship Program for Japanese Scholars and Researchers to Study Abroad (MEXT: Ministry of Education, Culture, Sports, Science and Technology).

References

[1] Th. Wacker, G.A. Sierra, A. Schweiger, The concept of FID-detected hole-burning in pulsed EPR spectroscopy, Isr. J. Chem. 32 (1992) 305–322.
[2] S.A. Dzuba, Y. Kodera, H. Hara, A. Kawamori, The use of selective hole-burning in EPR-spectra to study spectral diffusion and dipolar broadening, J. Magn. Reson. A 102 (1993) 257–260.
[3] Y. Kodera, S.A. Dzuba, H. Hara, A. Kawamori, Distances from tyrosine D+ to the manganese cluster and the acceptor iron in photosystem II as determined by selective hole-burning in EPR-spectra, Biochim. Biophys. Acta 1186 (1994) 91–99.
[4] Th. Wacker, A. Schweiger, Fourier-transform EPR-detected NMR, Chem. Phys. Lett. 186 (1991) 27–34.
[5] Th. Wacker, A. Schweiger, Fourier-transform hyperfine spectroscopy, Chem. Phys. Lett. 191 (1992) 136–141.
[6] H. Blok, J.A.J.M. Disselhorst, S.B. Orlinskii, J. Schmidt, A continuous-wave and pulsed electron spin resonance spectrometer operating at 275 GHz, J. Magn. Reson. 166 (2004) 92–99.
[7] H. Blok, J.A.J.M. Disselhorst, H. van der Meer, S.B. Orlinskii, J. Schmidt, ENDOR spectroscopy at 275 GHz, J. Magn. Res. 173 (2005) 49–53.
[8] M. van de Kamp, F.C. Hali, N. Rosato, A. Finazzi Agro, G.W. Canters, Purification and characterization of a nonreconstitutable azurin, obtained by heterologous expression of the *Pseudomonas-aeruginosa* asu gene in *Escherichia-coli*, Biochim. Biophys. Acta 1019 (1990) 283–292.
[9] A. Potapov, D. Goldfarb, The Mn^{2+}-bicarbonate complex in a frozen solution revisited by pulse W-band ENDOR, Inorg. Chem. 47 (2008) 10491–10498.